Demonstration of a low $V_\pi L$ modulator with GHz bandwidth based on electro-optic polymer-clad silicon slot waveguides

R. Ding[1,*], T. Baehr-Jones[1,5], Y. Liu[1], R. Bojko[1], J. Witzens[1], S. Huang[2], J. Luo[2], S. Benight[3], P. Sullivan[3], J-M Fedeli[4], M. Fournier[4], L. Dalton[3], A. Jen[2], and M. Hochberg[1]

[1]*Department of Electrical Engineering, University of Washington, Campus Box 352500, Seattle, WA 98195, USA*
[2]*Department of Materials Science and Engineering, Campus Box 352120, University of Washington, Seattle, WA 98195, USA*
[3]*Department of Chemistry, University of Washington, 109 Bagley Hall Box 351700, Seattle WA 98195, USA*
[4]*CEA LETI, Minatec 17 rue des Martyrs, 38054 Grenoble, France*
[5]*baehrjt@washington.edu*
**dingran@uw.edu*

Abstract: We demonstrate a near-infrared electro-optic modulator with a bandwidth of 3 GHz and a $V_\pi L$ figure of merit of 0.8 V-cm using a push-pull configuration. This is the highest operating speed achieved in a silicon-polymer hybrid system to date by several orders of magnitude. The modulator was fabricated from a silicon strip-loaded slot waveguide and clad in a nonlinear polymer. In this geometry, the electrodes form parts of the waveguide, and the modulator driving voltage drops across a 200 nm slot.

OCIS codes: (040.6040) Silicon; (060.4080) Modulation; (130.0130) Integrated Optics; (130.2790) Guided Waves; (130.3120) Integrated Optics Devices; (160.5470) Polymers.

References and links

1. T. Baehr-Jones, and M. Hochberg, "Polymer Silicon Hybrid Systems: A Platform for Practical Nonlinear Optics," J. Phys. Chem. C **112**(21), 8085–8090 (2008).
2. J. Leuthold, W. Freude, J.-M. Brosi, R. Baets, P. Dumon, I. Biaggio, M. L. Scimeca, F. Diederich, B. Frank, and C. Koos, "Silicon Organic Hybrid Technology-A Platform for Practical Nonlinear Optics," Proc. IEEE **97**(7), 1304–1316 (2009).
3. C. Koos, P. Vorreau, P. Dumon, R. Baets, B. Esembeson, I. Biaggio, T. Michinobu, F. Diederich, W. Freude, and J. Leuthold, "Highly-nonlinear silicon photonics slot waveguide," OFC **2008**, PDP25 (2008).
4. T. Baehr-Jones, B. Penkov, J. Huang, P. Sullivan, J. Davies, J. Takayesu, J. Luo, T.-D. Kim, L. Dalton, A. Jen, M. Hochberg, and A. Scherer, "Nonlinear polymer-clad silicon slot waveguide modulator with a half wave voltage of 0.25 V," Appl. Phys. Lett. **92**(16), 163303 (2008).
5. C. Koos, P. Vorreau, T. Vallaitis, P. Dumon, W. Bogaerts, R. Baets, B. Esembeson, I. Biaggio, T. Michinobu, F. Diederich, W. Freude, and J. Leuthold, "All-optical high-speed signal processing with silicon organic hybrid slot waveguides," Nat. Photonics **3**(4), 216–219 (2009).
6. V. R. Almeida, Q. F. Xu, C. A. Barrios, and M. Lipson, "Guiding and confining light in void nanostructure," Opt. Lett. **29**(11), 1209–1211 (2004).
7. Mach-40 intensity modulator *http://www.covega.com*
8. J. Wülbern, J. Hampe, A. Petrov, M. Eich, J. Luo, A. Jen, A. Falco, T. Krauss, and J. Bruns, "Electro-optic modulation in slotted resonant photonic crystal heterostructures," Appl. Phys. Lett. **94**(24), 241107 (2009).
9. A. Liu, R. Jones, L. Liao, D. Samara-Rubio, D. Rubin, O. Cohen, R. Nicolaescu, and M. Paniccia, "A high-speed silicon optical modulator based on a metal-oxide-semiconductor capacitor," Nature **427**(6975), 615–618 (2004).
10. T. Baehr-Jones, M. Hochberg, G. Wang, R. Lawson, Y. Liao, P. Sullivan, L. Dalton, A. Jen, and A. Scherer, "Optical modulation and detection in slotted Silicon waveguides," Opt. Express **13**(14), 5216–5226 (2005).
11. D. Chen, H. R. Fetterman, A. Chen, W. H. Steier, L. R. Dalton, W. Wang, and Y. Shi, "Demonstration of 110 GHz electro-optic polymer modulators," Appl. Phys. Lett. **70**(25), 3335–3337 (1997).
12. M. Lee, H. E. Katz, C. Erben, D. M. Gill, P. Gopalan, J. D. Heber, and D. J. McGee, "Broadband modulation of light by using an electro-optic polymer," Science **298**(5597), 1401–1403 (2002).
13. J. Witzens, T. Baehr-Jones, and M. Hochberg, "Design of transmission line driven slot waveguide Mach-Zehnder interferometers and application to analog optical links," Opt. Express (to be published).

#128427 - $15.00 USD Received 17 May 2010; revised 28 Jun 2010; accepted 28 Jun 2010; published 8 Jul 2010

14. S. J. Spector, M. W. Geis, G.-R. Zhou, M. E. Grein, F. Gan, M. A. Popovic, J. U. Yoon, D. M. Lennon, E. P. Ippen, F. Z. Kärtner, and T. M. Lyszczarz, "CMOS-compatible dual-output silicon modulator for analog signal processing," Opt. Express **16**(15), 11027–11031 (2008).
15. D. Gill, S. Patel, M. Rasras, K.-Y. Tu, A. White, Y.-K. Chen, A. Pomerene, D. Carothers, R. Kamocsai, C. Hill, and J. Beattie, "CMOS-Compatible Si-Ring-Assisted Mach–Zehnder Interferometer With Internal Bandwidth Equalization," IEEE J. Quantum Electron. **16**(1), 45–52 (2010).
16. W. M. J. Green, M. J. Rooks, L. Sekaric, and Y. A. Vlasov, "Ultra-compact, low RF power, 10 Gb/s silicon Mach-Zehnder modulator," Opt. Express **15**(25), 17106–17113 (2007).
17. L. Liao, A. Liu, D. Rubin, J. Basak, Y. Chetrit, H. Nguyen, R. Cohen, N. Izhaky, and M. Paniccia, "40 Gbit/s silicon optical modulator for highspeed applications," Electron. Lett. **43**(22), 1196–1197 (2007).
18. R. A. Soref, and B. R. Bennett, "Electrooptical effects in silicon," IEEE J. Quantum Electron. **23**(1), 123–129 (1987).
19. H. F. Okorn-Schmidt, "Characterization of silicon surface preparation processes for advanced gate dielectrics," IBM J. Res. Develop. **43**(3), 351–365 (1999).
20. T. Baehr-Jones, Department of Electrical Engineering, University of Washington, Campus Box 352500, Seattle, WA 98195, R. Ding, Y. Liu, R. Bojko, J-M. Fedeli, and M. Hochberg are preparing a manuscript to be called "Low-Loss Strip-loaded slot waveguides in Silicon-on-Insulator."
21. J. Luo, X.-H. Zhou, and A. K.-Y. Jen, "Rational molecular design and supramolecular assembly of highly efficient organic electro-optic materials," J. Mater. Chem. **19**(40), 7410–7424 (2009).
22. D. M. Beggs, M. Ayre, D. F. G. Gallagher, and T. F. Krauss, "Design and fabrication of high-efficiency fibre couplers for nanophotonic devices," Microelectron. Eng. **84**(5-8), 1446–1449 (2007).
23. M. Hochberg, T. Baehr-Jones, G. Wang, J. Huang, P. Sullivan, L. Dalton, and A. Scherer, "Towards a millivolt optical modulator with nano-slot waveguides," Opt. Express **15**(13), 8401–8410 (2007).

1. Introduction

The silicon-polymer hybrid platform [1–3] shows great potential for a number of applications, including building low drive-voltage modulators [4] and high-speed all-optical switches [5]. Recently, a slot-waveguide [6] based silicon waveguide clad in an electro-optic polymer has been used to build a modulator with a V_π of 0.25 V [4], approximately a factor of 20 lower than a typical commercial modulator [7]. Photonic crystal – slot waveguide hybrid devices have also been demonstrated [8]. However, in all cases, the results have been at slow speeds, on the order of 1 kHz.

All-silicon-based electro-optic modulators rely on the modulation of charge density, in which the process of carrier injection and removal limits the speed [9]. However, the second-order nonlinear moment of electro-optic polymers is believed to be ultrafast [10], and modulators that can operate at frequencies higher than 100 GHz have in fact already been demonstrated [11,12]. For polymer-silicon hybrid systems, the silicon contacts only act as transparent electrodes, and so carrier drift velocities are not a fundamental limitation. There is therefore the potential that polymer-silicon modulators could perform at speeds not only on the order of 10 GHz, but could eventually perform at speeds in the 100 GHz regime or higher [13]. But to our knowledge no high-speed electro-optic modulation results have yet been shown in silicon–polymer hybrid system.

Here, we demonstrate a polymer-clad silicon slot waveguide that can work in the gigahertz regime. Our device is relatively short, at only 1 mm, and so the V_π is relatively large at 8 V. The $V_\pi L$ figure of merit for this modulator is 1.6 V-cm (single-ended), and 0.8 V-cm (push-pull) [14,15], which is within a factor of 2 of the figure of merit used achieved by the 0.25 V V_π result [4]. This demonstrates that the same low drive voltages achieved at slow speeds are likely to eventually be realized in RF bandwidth devices.

While $V_\pi L$ values of 0.036 V-cm have been achieved with forward-biased p-i-n diode modulators [16], the need for a bias voltage creates a number of problems, and drives power consumption. Additionally, modulators based on this technique will likely be ill-suited for analog applications requiring high linearity. Unbiased, highly linear, Lithium-Niobate modulators are still a dominant technology for high-performance optical modulation. Silicon modulators that do not require bias, and can operate at higher speeds, have typical $V_\pi L$ values of 4 V-cm [17].

#128427 - $15.00 USD Received 17 May 2010; revised 28 Jun 2010; accepted 28 Jun 2010; published 8 Jul 2010

2. Design and fabrication

The configurations as well as an SEM micrograph of the "strip-loaded" slot waveguide used in the device are shown in Fig. 1. A thin silicon strip, so called "strip-loading", is used to make electrical contact from the metal pad to each arm of the slot waveguide. In this specific device, the waveguide dimensions are 200 nm silicon thickness, 300 nm arm width, and 200 nm slot width, the modal pattern near 1550 nm as shown in Fig. 1(a). A very conservative 10 μm metal-to-waveguide clearance was used to allow for fabrication error and avoid excess optical loss.

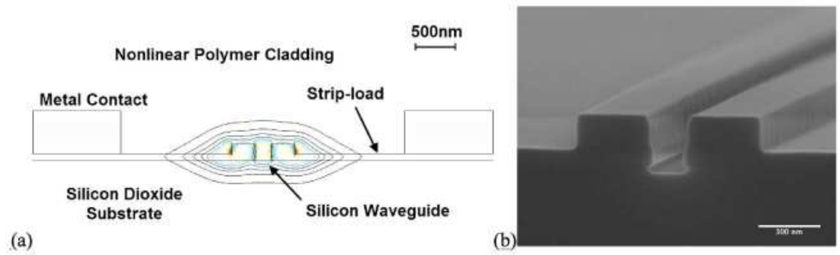

Fig. 1. (a) The diagram of the silicon slot waveguide as used in the Mach-Zehnder modulator described in this work. The modal pattern near 1550nm is plotted; contours of $|E_x|$ are shown (x-axis is assumed to be parallel to the substrate and perpendicular to the propagation direction). (b) SEM micrograph of the cross-section of a strip-loaded slot waveguide.

To achieve high-bandwidth modulation, low-resistance electrical contact between the slot arms and the driving electrodes must be made to avoid a large RC time constant, thus the thickness and doping of the strip-loading region are important considerations. A tradeoff between optical loss and electrical conductivity needs to be made to determine the doping concentration [18]. Making the strip-loading thicker will naturally decrease the resistance in accordance with Ohm's law, although the process of waveguide design will become more challenging.

A further consideration is the surface states that are frequently created in the course of processing silicon. For a surface terminated by a chemical oxide, the surface state density is about 10^{12} cm^{-2} [19]. This density of surface states will "pin" the Fermi-level, depleting the near surface region, making the effective height of the arms for current flow less than the physical height of the silicon. Therefore, we chose a relatively thick strip-loading as 70 nm to accommodate various doping concentrations.

A Mach–Zehnder modulator was built using this geometry of waveguide, and the device layout is shown in Fig. 2. The fabrication of the slot waveguides was done with two self-aligned photolithography steps on a 193 nm stepper and two Si dry etching steps on Silicon-On-Insulator (SOI) wafers (having 220 nm thick silicon layer, 2 μm thick buried oxide layer and substrate resistivity of 10 Ω-cm). Thin thermal oxide was employed to smoothen the waveguide sidewalls [20]. This oxide was stripped by buffered oxide etch (BOE) before metallization. The chip was uniformly 10^{18} cm^{-3} Boron doped (resistivity was anticipated as 0.04 Ω-cm) and annealed after fabrication. The metallization process was done by contact photolithography and the pads were formed by Al evaporated and lift-off process. Before polymer coating, a 10min anneal at 460 °C was performed to enhance metal-semiconductor contact since there was no contact implant step.

#128427 - $15.00 USD Received 17 May 2010; revised 28 Jun 2010; accepted 28 Jun 2010; published 8 Jul 2010

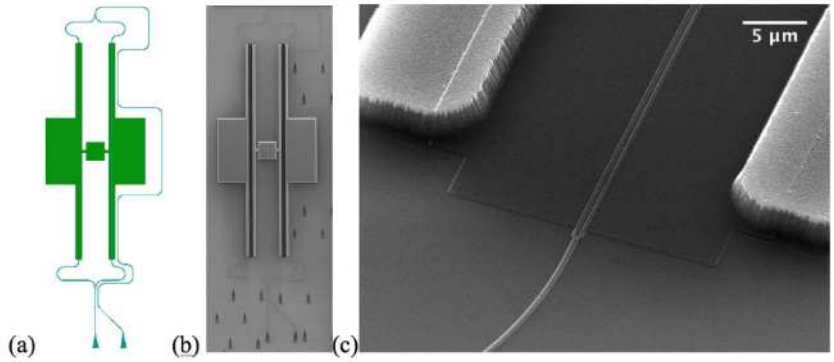

Fig. 2. (a) Mach-Zehnder modulator layout; (b) SEM micrograph showing the fabricated device; (c) SEM micrograph of the layout of one arm showing the region where ridge waveguide couples into strip-loaded slot waveguide and metal pads sitting on strip-loading.

The AJSP-series electro-optic polymers are newly developed high-efficiency nonlinear optical materials, and their r_{33} values range from 50 to 200 pm/V at telecommunication wavelengths [21]. AJSP100 exhibits relatively large electro-optic activity (r_{33} value of ~65 pm/V at 1550 nm), low optical loss (~1 dB/cm), and good temporal and photochemical stability, and it is suitable for a broad spectrum of photonic applications. The electro-optic polymer cladding was prepared by doping AJSP100 into PMMA host and the resultant refractive index of the polymer was 1.54 at 1550 nm. A poling field of 100 V/μm and poling temperature of 103 °C were used. During the poling the center pad was set to 0 V, left pad was set to + V_{pole} and right pad was set to $-V_{pole}$, where V_{pole} = 20 V to achieve the poling field across a 200 nm slot. During modulation, the center pad was set to signal while the left and right pads were held at ground, so that the modulator was operated in a push-pull fashion.

3. Measurement results

Grating couplers were used to couple light on and off the chip [22], which had a 3-dB bandwidth of around 35 nm. Total device insertion losses were approximately –44 dB fiber to fiber.

3.1 DC V_π

Figure 3 shows device transmission spectra for various DC drive voltages, which was applied to the center pad of the device while the side pads being held at ground. Because this data is for an unbalanced Mach–Zehnder with arm lengths of 1mm and 1.08 mm, there is an approximately 7 nm periodicity in the transmission as a function of wavelength. The more gradual variation is from the grating coupler bandwidth. The half-wave voltage V_π can be roughly determined as 8 V, from the plots, which corresponds to a $V_\pi L$ of 0.8 V-cm. Due to the strip-loading, the optical mode was less confined as compared to that of a slot waveguide without strip-loading, and the 200 nm relatively wide slot further lowered the effective index susceptibility [23], which turned out to be only 0.2 μm^{-1}. Thus, 0.8 V-cm $V_\pi L$ suggested that an in-device poled r33 of 40 pm/V was achieved.

#128427 - $15.00 USD Received 17 May 2010; revised 28 Jun 2010; accepted 28 Jun 2010; published 8 Jul 2010

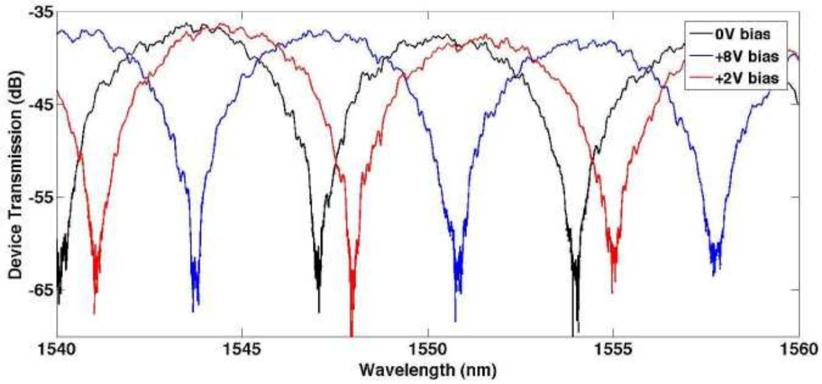

Fig. 3. Transmission through the Mach–Zehnder device as a function of wavelength, for various modulator drive voltages. As can be seen, 2 V bias suggested the direction of spectrum shift, 8 V bias was slightly above V_π voltage.

3.2 Frequency response

The unbalanced Mach-Zehnder design allow us to bias the modulator at a $\pi/2$ bias point, corresponding to 3 dB of extinction and the maximum response to a driving voltage, by setting the signal wavelength to the appropriate value. The frequency response of the device was characterized from 200 Hz to 2 GHz.

A vector network analyzer (VNA) was used to drive the modulator from port 1, with a New Focus 1647 1.1 GHz bandwidth avalanche photodiode (APD) converting the optical response to RF, which was directed to port 2. Data was taken from 20 MHz to 2 GHz with this setup. Then, a New Focus 1414 25 GHz high-speed photodetector was used instead of the APD to take data from 100 MHz up to 6 GHz. It can readily be shown that the S21 parameter is directly related to the V_π value of the modulator when the modulator is biased at the −3 dB point, so as to be in a linear operating regime. The typical signal to noise ratio encountered in this measurement was 30 dB. As the modulator was expected to have high impedance, we assumed that the drive voltage was doubled on the actual device.

For the frequency range from 200 Hz to 100 MHz, a function generator was used to drive the modulator with a sinusoidal signal with peak-to-peak voltage of 2 V. A DC lock-in amplifier and an RF lock-in amplifier were used to characterize the signal output by the photodetector, which was a Thorlab DET01CFC. The results are shown in Fig. 4 as normalized S21. The corresponding normalized S21 of 8 V V_π is also plotted on the same axes. The S21 measurement from each detector was renormalized as well for the detector gain and the laser power level, so as to allow direct comparisons between different measurements. Typical noise floors were at least 10 dB beneath the measurement, and often substantially lower. The noise floor during the measurement with the high-speed detector is plotted in Fig. 4. Since the high-speed photodetector only has a peak gain of 0.6 A/W, and the VNA has a lower dynamic range in low frequency band, the data taken with the high-speed photodetector is not presented for the frequency range from 100 MHz to 200 MHz due to the low signal-to-noise ratio.

From the spectrum of S21, we observed that the flatness of the response extended from DC to gigahertz range, and the absolute value of S21 corresponded very well to the value implied by 8 V V_π. 6 dB rolloff point occurred at around 3 GHz. It should be noted that our 6 dB rolloff in S21 corresponds to a 3 dB in the optical response typically defined to characterize modulator bandwidth as used by Liu *et al* [9].

The capacitance of each arm can be estimated as 80 pF/m if we assume the polymer has a RF dielectric constant of 4 [13]. When combined with the arm resistance, which is roughly 70 Ω from each pad to the waveguide arm (assuming fully-charged surface states, thus 10nm silicon depletion region at this doping), one would expect to see a device bandwidth on the order of 15 GHz. So, our observed bandwidth was significantly lower than the predicted

#128427 - $15.00 USD Received 17 May 2010; revised 28 Jun 2010; accepted 28 Jun 2010; published 8 Jul 2010

value. This is less likely due to RF attenuation or velocity mismatch considering the short length of the device. One possible source of the limitation is a higher than expected resistance in the strip-loading section. Considering the buffered-oxide etching step mentioned in Section 2, the removal of passivation oxide by wet etching could generate considerably higher density of surface states in silicon as opposed to those terminated with high quality gate oxide [19]. It is also possible that there is parasitic resistance in the metal pad contacts, which could be explained by the lack of a high dose contact implant, or could be caused by mechanical damage to the pads during poling or testing. RF coupling to the substrate is another possible source of the rolloff – the pads are large and the silicon substrate beneath the buried-oxide layer is not highly resistive. Further design and experimental work is expected to increase the bandwidth of these devices greatly.

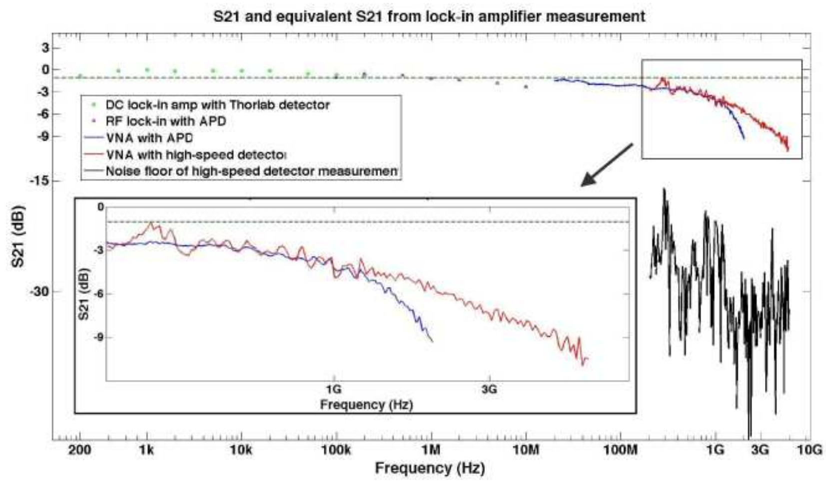

Fig. 4. The frequency dependence of the device: 6 dB rolloff in S21 occurred around 3 GHz. The corresponding normalized S21 of 8 V V_π is also plotted in the same axis. The inset graph shows the response from 200 MHz to 6 GHz, in which the −6 dB rolloff appears around 3 GHz.

4. Conclusion

We have presented an electro-optic modulator based on nonlinear optical polymer and strip-loaded slot waveguide, demonstrating that polymer-clad silicon slot waveguides can work in gigahertz regime while maintaining low $V_\pi L$. Our measurements indicated a figure of merit $V_\pi L$ of 0.8 V-cm and a bandwidth of 3 GHz.

There are several options to improve the device performance. One possibility is reducing the metal to waveguide clearance; if the resistance in the strip-loaded section is the limitation, and this spacing were reduced to one third of its current value, the bandwidth would likely increase to 10 GHz, while adding very negligible optical loss according to finite-difference-time-domain simulation. Additionally, instead of heavily doping the chip uniformly, doping the waveguide lightly while doping the proximity of the waveguide heavily would decrease the optical loss, but lower the series resistance from metal contact to the waveguide. We believe that device performance can be dramatically improved, with eventual bandwidths of 100 GHz achievable in a 1 mm device [13].

Acknowledgments

The authors would like to thank Gernot Pomrenke, of the Air Force Office of Scientific Research, for his support through an AFOSR Young Investigators Program Grant, FA9550-08-1-0101, and would like to acknowledge support from the NSF STC MDITR Center, DMR0120967 and the Washington Research Foundation. A. Jen would like to gratefully acknowledge support from the Office of Naval Research. The authors would also like to thank Jay VanDelden of Eigenphase Technologies.